Marine Genomics 20 (2015) 45–55

Contents lists available at ScienceDirect

Marine Genomics

journal homepage: www.elsevier.com/locate/margen

Transcriptomic response to shell damage in the Antarctic clam, *Laternula elliptica*: Time scales and spatial localisation

Victoria A. Sleight *, Michael A.S. Thorne, Lloyd S. Peck, Melody S. Clark

British Antarctic Survey, Natural Environment Research Council, High Cross, Madingley Road, Cambridge, CB3 0ET, UK

ARTICLE INFO

Article history:
Received 23 December 2014
Received in revised form 30 January 2015
Accepted 30 January 2015
Available online 9 February 2015

Keywords:
Biomineralisation
Mantle
Calcification
Gene expression
Repair

ABSTRACT

Mollusc shell is built-up by secretion from the mantle and is the result of a controlled biological process termed biomineralisation. In general mollusc shells are well characterised however, the molecular mechanisms used by molluscs to produce shell remain largely unknown. One tractable method to study molecular biomineralisation mechanisms are shell damage-repair experiments, which stimulate calcification pathways. The present study used the Antarctic clam (*Laternula elliptica*) as a model to better understand when and where molecular biomineralisation events occur in the mantle. Two approaches were used: one experiment used high-throughput RNA-sequencing to study molecular damage-repair responses over a 2 month time series, and a second experiment used targeted semi-quantitative PCR to investigate the spatial location of molecular mechanisms in response to damage. Shell repair in *L. elliptica* was slow, lasting at least 2 months, and expression results revealed different biological processes were important at varying time scales during repair. A spatial pattern in relation to a single drilled hole was revealed for some, but not all, candidate genes suggesting the mantle may be functionally zoned and can respond to damage both locally and ubiquitously across the mantle. Valuable data on the temporal and spatial response of shell damage-repair provide a baseline not only for future studies in *L. elliptica*, but also other molluscs.

1. Introduction

The Mollusca is a diverse, speciose and successful phylum made up of an estimated 85,000 extant species (Appeltans et al., 2012; Lydeard et al., 2004). Molluscs are essential in worldwide ecosystem functioning, as well as representing an increasing food supply for the growing human population. The success of the molluscan phylum is often attributed to the possession of a shell (Marie et al., 2013; Vermeij, 2005). Shells are multifunctional structures; they provide critical protection to the soft-bodied animal within, support for internal anatomy, and a means by which the animal can seal itself off from the environment (Wilbur and Saleuddin, 1983). Currently there is interest in the structure of shells and their manufacture from diverse fields of science. Environmental biologists are concerned about the ecological fate of calcified structures as the oceans become more acidic. There is therefore, a requirement to understand the calcification pathway in order to inform predictions on how ecosystems might alter with climate change (Gazeau et al., 2013). Material scientists are also interested in biomineralisation for multiple reasons. The high strength of shell, compared to other composite materials, makes it an attractive solution to meet the demand for low-energy, solid materials formed from abundant soluble calcium carbonate (Meldrum, 2003). In addition, understanding biomineralisation introduces the prospect of engineering products such as mother of pearl and pearls without the need for a live animal (Arnaud-Haond et al., 2007).

The molluscan shell is laid down by the mantle and is the result of a controlled biological process (termed biomineralisation). Shells typically contain 95-99% calcium carbonate ($CaCO_3$) and 1-5% organic matrix. In general molluscan shells are well characterised in terms of morphology and microstructure (de Paula and Silveira, 2009; Weiner and Addadi, 2011) however, further study is required to understand the precise molecular processes used to produce shell from soluble calcium carbonate. Early work showed that proteins are secreted into a matrix structure which applies antagonistic forces to either nucleate or inhibit crystal growth (Meenakshi et al., 1971; Weiner and Hood, 1975). There is also an increasing body of work identifying proteins in shell matrices (Joubert et al., 2010; Marie et al., 2012; Miyamoto et al., 2005) and genes in mantle tissues, which may be involved in biomineralisation (Clark et al., 2010; Freer et al., 2014; Niu et al., 2013; Shi et al., 2013). Normal shell growth is a costly metabolic process (Palmer, 1992); shell production is a background process with gene (and protein) expression levels in the mantle likely to be low in abundance and therefore difficult to detect. One tractable method to highlight biomineralisation molecular mechanisms are shell damage-repair experiments that stimulate calcification pathways (Clark et al.,

* Corresponding author. Tel.: +44 1223 221288.
E-mail address: viceig15@bas.ac.uk (V.A. Sleight).

http://dx.doi.org/10.1016/j.margen.2015.01.009

2013b; Mount et al., 2004). Previous shell damage-repair studies are largely single time point or short-term experiments that provide a proof of concept that damage-repair is a useful method to understand biomineralisation. Currently however, the temporal and spatial components of shell damage-repair experiments are lacking for shelled molluscs.

The present study used the Antarctic clam (*Laternula elliptica*) as a model to better understand when and where molecular biomineralisation events occur. *L. elliptica* is an important species in the Southern Ocean ecosystem, where it is one of the most abundant animals (in terms of live biomass) and plays an important role in coupling pelagic and benthic systems through nutrient cycling (Arntz et al., 1994). As a species, *L. elliptica* faces major environmental challenges under future climate change. The Southern Ocean is predicted to soon become undersaturated in calcium carbonate in ocean acidification models; some model scenarios predict aragonite will be undersaturated by 2030 (McNeil and Matear, 2008). In addition, the Western Antarctic Peninsula region is experiencing one of the fastest rates of warming on the planet (Turner et al., 2014). A consequence of the latter, aside from the temperature rise *per se*, is an increase in ice calving events and iceberg scouring which can decimate sea beds and the associated infaunal communities (Cook et al., 2005). In the face of changing conditions, *L. elliptica* often survive iceberg damage and exhibit considerable morphological shell plasticity in response to environmental cues (Harper et al., 2012). *L. elliptica* represents a highly tractable mollusc model for studying biomineralisation processes at low temperatures (circa 0 °C).

The objectives of the present study are: 1.) To better understand the timing of biomineralisation in response to damage. 2.) To identify candidate biomineralisation genes involved in response to damage. 3.) To understand the spatial location of molecular mechanisms in response to damage.

2. Materials and methods

2.1. Animals

Laternula elliptica specimens were collected by SCUBA divers from Hangar Cove near Rothera Research Station, Adelaide Island Antarctic Peninsula (67° 34' 07" S, 68° 07' 30" W) at depths of 10–15 m. Animals were immediately returned to the laboratory where they were maintained in a flow-through aquarium with temperature of 0.6 ± 0.3 °C, under a 12:12 simulated natural light:dark cycle. Animals were transferred to the British Antarctic Survey aquarium facilities in Cambridge, UK. In Cambridge, all animals were habituated to aquarium conditions for at least four weeks (closed water system at water temperature and salinity of 0 ± 0.5 °C and 35–38 ppt respectively, 12 h:12 h light:dark, fed algal culture weekly) prior to experimentation.

Two independent shell damage experiments were carried out to investigate both the timing of repair mechanisms and the spatial localisation of the repair response.

2.2. Experiment one: transcriptional profiling of damage response during a time series

2.2.1. Experimental design

Experiment one investigated the timing of molecular biomineralisation responses and was carried out over a two month time course. Half of the animals in the experiment were damaged (n = 14, mean shell length = 27.2 mm ± 1.2 S.E.), while the other half were left undamaged (n = 14, mean shell length = 23.97 mm ± 0.56 S.E.). Damage was inflicted by drilling a hole through the shell (just inside the pallial line close to the ventral edge of the shell and so within reach of the mantle margin), using a 10.8 V Lithium-Ion Dremel cordless modelling drill (model 800, variable speed, 5,000 - 35,000 rpm) fitted with a round-tipped bur to minimise any trauma to the underlying soft tissue. Samples of mantle tissue were subsequently taken at three time points: 1 week, 1 month and 2 months (n = 4–6 for each of the control and damaged treatments). Mantle tissues were dissected from each individual from directly under the drilled hole (or equivalent location in control animals), across the three mantle folds, snap frozen in liquid nitrogen and stored at −80 °C prior to RNA extraction.

2.2.2. RNA extraction and sequencing

Total RNA was extracted from the mantle tissue of each animal on ice using Tri-Reagent (Sigma-Aldrich, UK) according to manufacturer's instructions, and purified using RNeasy columns (QIAGEN, UK). All RNA samples were analysed for concentration and quality by spectrophotometer (NanoDrop, ND-1000) and tape station analyses (Agilent 2200 TapeStation). RNA samples from 4–6 individuals were pooled for each treatment and time point to make a total of 6 libraries (1 week control and damaged; 1 month control and damaged and 2 months control and damaged). TruSeq libraries were produced and subjected to 100 bp paired-end read sequencing on an Illumina Hi-Seq 2000 by The Genome Analysis Centre (TGAC, Norwich).

2.2.3. Bioinformatics and statistics

A bioinformatic pipeline was developed to analyse the RNA–Seq data. The paired-end Illumina reads were assembled into a *de novo* transcriptome using Soapdenovo with default parameters (Luo et al., 2012). The newly assembled experimental transcriptome was combined with the previously published *L. elliptica* transcriptome (Clark et al., 2010), to produce a total of 43,356 contigs. All contigs were compared to the NCBI non-redundant (nr) database using Basic Local Alignment Search Tool (BLAST) to search for sequence similarity and putative gene annotation (Altschul et al., 1990). The paired-end reads from each experimental treatment were mapped to the transcriptome using Maq with default parameters (Li et al., 2008).

DEXUS (a Bioconductor package available for R that assumes read counts as a finite mixture of negative binomial distributions) was used with default parameters (including default normalisation) to detect differential expression between control and damaged treatments at each time point (Klambauer et al., 2013). DEXUS uses a Bayesian approach to provide evidence of differential expression measured by the informative/noninformative (*I/NI*) value. The top 50 annotated, differentially expressed contigs for each time point were used for further analysis. Putative annotations were confirmed manually using Blastx against both the Uniprot human database and the NCBI nr database. In addition, seven "classic" candidate biomineralisation genes were selected using keyword searches and tracked through the DEXUS analysis.

To provide a visual qualitative assessment of the differential biological processes at each time point, STRING v9.1 program was used (Franceschini et al., 2013). The UniProt human annotations for the top 50 annotated differentially expressed contigs were entered into the STRING program. Using the protein-protein interactive network mode in STRING, all non-interacting proteins were removed from analysis and the remaining interactions were clustered using Markov cluster algorithm (MCL).

The RNA-Seq Illumina reads from the current project have been submitted to the NCBI SRA (Sequence Read Archive), BioProject accession number: PRJNA268918. The updated assembled contig dataset, using the previously published and the current experimental *L. elliptica* data, is available for download from the Polar Data Centre (http://tinyurl.com/l5uvczh).

2.3. Experiment two: localisation of damage response

2.3.1. Experimental design

Experiment two investigated the spatial location of molecular events and was carried out over 1 week using two treatments; damaged (method as in Section 2.2, n = 5, mean shell length = 68.2 mm ± 1.07 S.E.) and undamaged control (n = 5, mean shell length = 66.4 mm ±

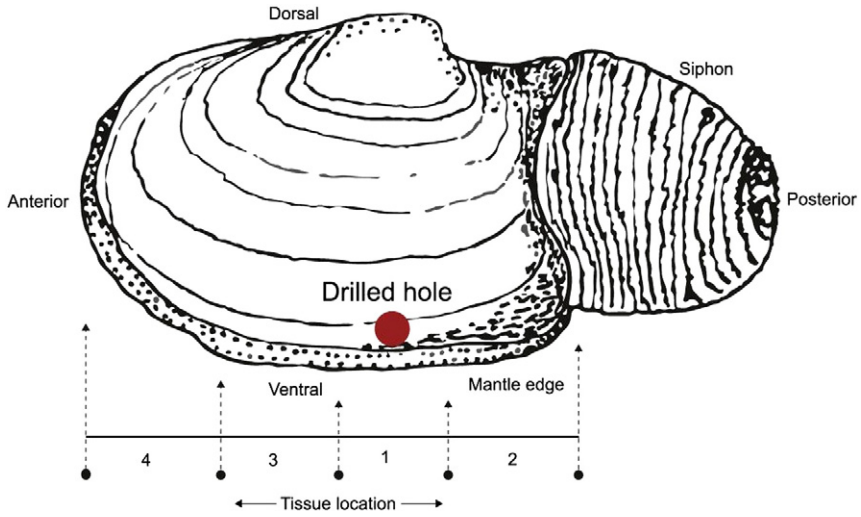

Fig. 1. Schematic diagram showing the site of damage and the localisation sampling protocol in experiment two. Two tissue samples were taken from each tissue location. Image not to scale.

3.06 S.E.). Animals in experiment two were larger/older than experiment one in order to maximise the spatial distance between the areas of the mantle sampled. After 1 week, animals were sacrificed and mantle tissues were dissected into four regions, with two samples taken from each region (Fig. 1). Tissue samples were snap frozen in liquid nitrogen and stored at −80 °C prior to RNA extraction.

2.3.2. Semi-quantitative PCR (semi-Q PCR)

Total RNA was extracted from each section of mantle tissue of individual animals (n = 5) and quantified as described in Section 2.2. Semi-Q PCR was carried out as per Zhou et al., 2010 with minor modifications optimising for primer specific annealing temperatures and cycle number. All samples were diluted to 30 ng μl^{-1} total RNA prior to reverse transcription. Following a DNase step, cDNA was synthesized from 1 μg RNA using manufacturer's protocol (Qiagen, QuantiTect Reverse Transcription Kit). cDNA was stored at −80 °C until gene expression analysis.

A total of twelve candidate biomineralisation genes were selected to investigate the localisation of the repair response within the mantle tissue (Table 1). Candidates comprised eight highly expressed transcripts selected from the previously published *L. elliptica* transcriptome (Clark et al., 2010), including three which had no putative annotation assigned by sequence similarity searching, but which were determined to have a mantle-specific expression (Vieira, pers comm) and were present in a shell proteome analysis (Marie, pers comm.). Four additional transcripts, which were highly up-regulated in response to damage after 1 week in experiment one, were also included. Gene-specific primers were designed for each candidate using the Primer 3 software (http://frodo.wi.mit.edu/) to produce single amplicons with a size of approximately 200–400 bp, annealing temperature of 57–60 °C

Table 1
Candidate genes of interest selected from previous transcriptome and proteome studies, annotation and primers used in semi-Q PCR. NA = no significant match, *L. elliptica* 18 s = housekeeping gene for normalisation.

Contig I.D.	Sequence similarity (BLAST)/domains (Conserved Domain Database(CDD))	Putative function	Forward and reverse Primer sequence (5' → 3')	Amplicon size	Annealing temperature (°C)
L. elliptica 18 s	*L. elliptica* 18 s	*L. elliptica* 18 s	GGCCGTTCTTAGTTGGTGGA TCATTAACTGGGGCGATCGG	447	60
Contig 02037	Astacin-like/Zinc metalloprotease domain	Anti-microbial/Immune	GAAAACGCCCGACTTGAATA TCGGTGTGACATCGTTTGAT	496	58
Contig 00332	Pif/2 trombospondin + 2 chitin-binding domains	Biomineralisation/Immune	GGACAACACATTGGGGTAGG GGATGTATCGGGGAAAAGGT	350	58
Contig 01359	Tyronsinase B/Tyrosinase Domain	Biomineralisation	CGGCCTCATCGTGATAATCT GGGAAGATTTTCGAATGCAA	479	58
Contig 01311	P86860/2 chitin-binding + Mucin + LamG domains with calcium mediated ligand binding site	Biomineralisation	CACTGTGCTTCGCTGAACAT GATCTACGCCCTCGTCAGAG	414	58
Contig 01785	Mytilin-3/NA	Immune	CGCCGATATGGATTTACGTG GGCGAGACAGAATTCGGATA	413	60
Contig 00041	NA/Chitin binding Peritrophin-A domain	Biomineralisation	TTTCGCCGCTAGAAGTGTGT GGGTTCGTCAACATCCAGGT	407	60
Contig 01043	NA/NA	NA	GGGTCAGCTGGTATCCTTGA AGCGCTTGCAAAATTGTCTT	457	60
Contig 01663	Tyronsinase A/Tyrosinase Domain	Biomineralisation	CCATCCGCTATCTGTGGTCC TCTTTTGCGACCTCAGACCC	399	60
Contig 18937102	Chitinase/NA	Biomineralisation/Immune	CGTTGGTGTAGGTTCCATTC GGCATGACCGGTATTAACAG	232	56
Contig 1586	Tyrosine/NA	Signalling/Biomineralisation	AGTTTTGTGCTGCCTTCAAC CACGTGTTTGTGCTCTTCAC	210	57
Contig 2930	NA/NA	NA	TTGAAGTGTTACGCCTCCTC AGCACTGCCTGGTGATAGAG	175	56
Contig 3459	NA/NA	NA	AAAATCAACGAGGAGGAGGA GGGAATCCAGGTCTCTCTGT	150	57

and GC content between 55–60%. PCR amplicons were sequenced to confirm identity.

cDNA was used as the template in PCR amplification for the twelve candidate genes and the *L. elliptica* 18 s gene was used as a positive control and reference housekeeping gene. PCR was carried out in a 43 μL reaction volume containing 0.5 μL cDNA, 23.5 μL H_20, 5 μL NH_4 10× buffer (Bioline, UK), 1.5 μL $MgCl_2$ (50 mM Bioline, UK), 5 μL deoxynucleoside triphosphates mix (Bioline, UK), 5 μL of each primer (10 mM, Invitrogen, UK) and 0.25 μL Taq polymerase (BioTAQ, Bioline, UK). Following initial denaturation at 95 °C for 5 min, twenty six PCR cycles were carried out as follows: denaturation at 95 °C for 15 s, primer specific annealing temperature for 20 s, and extension at 72 °C for 30 s. Amplified products were analysed by electrophoresis on 1.5% agarose gel (Bioline, UK) containing GelRed™ and visualized under UV illumination (U:genus 3; Syngene, Cambridge, UK). The relative intensities of amplified PCR products were determined using Syngene GeneTools software (version 3.06) and expressed as an integrated density value (IDV). Primer efficiency was optimised across a temperature gradient and for number of PCR cycles, as well as including serial dilutions to check that semi-quantification was achievable. Each round of PCR reactions included a no template control to check for contamination.

2.3.3. Statistical analyses

Integrated density values (IDVs) from the GeneTools analysis were manipulated into an index for gene expression, as well as normalised, by division using a housekeeping reference 18 s IDV. 18 s was confirmed as an appropriate housekeeping reference gene as there was no significant difference in IDV between samples. Gene expression data were not normal and could not be transformed to reach normality therefore, non-parametric statistical analyses were used. To test if the candidate gene was up or down regulated in response to damage, data from control and damaged treatments were compared using a Kruskal–Wallis one-way analysis of variance by ranks. To test if there was a spatial pattern in expression across the four mantle regions in response to damage, data within the control and damaged treatments were compared using a Kruskal–Wallis one-way analysis of variance by ranks. Where statistically significant differences were found ($p < 0.05$) a non-parametric, ranked-sum, post-hoc Tukey HSD test was used to identify differences between regions. Statistical analyses for experiment two were carried out using MiniTab 15 and MATLAB.

Candidate genes were also isolated from the DEXUS analysis in experiment one to investigate their expression over time. Thus providing data on both timing and localisation for a key set of contigs, as well as linking experiment one with experiment two.

3. Results

3.1. Experiment one: transcriptional profiling of damage response during a time series

The previously published, and new experimental transcriptome from the current study, were combined to make a total of 43,356 contigs. 32% of contigs were assigned putative functions using BLAST sequence similarity searching (below an e-value of $1e^{-10}$). Maq mapped transcripts to 42,807 (98.7%) contigs for differential gene expression analysis.

DEXUS analysis revealed differential expression between control and damaged groups, which varied over the time series (Table 2). 6046 transcripts (14.1% of total) were differentially expressed at week 1, the highest number of differentially expressed transcripts was at 1 month (7402; 17.3%) and the lowest was at the 2 month time point (2998; 7%).

At each time point, the top (annotated) differentially expressed contigs between control and damaged treatments were different (Supplementary Table 1, 2 and 3). Qualitative analysis using STRING indicated different biological processes were important at different time points (Fig. 2). Specifically, after 1 week, DNA repair, immune response, RNA processing, cytoskeleton and mitosis were the dominant differential processes. After 1 month, respiratory electron transport chain and cell cycle regulation were most prominent and after 2 months apoptosis, protein folding, mRNA splicing and protein regulation dominated the differentially expressed processes.

The "classic" biomineralisation genes remained generally unchanged over the time series (Table 3; Supplementary Table 4). After 1 week, only the *Insoluble matrix shell protein* showed differential expression between control and damaged treatments. After 1 month, only *PfN44* was differentially expressed and after 2 months, *Pif* and *Chitin synthase* were differentially expressed.

The twelve candidate genes of interest identified in experiment two were also specifically investigated in the DEXUS analysis (Table 4). Ten out of the twelve genes showed a time-dependant expression pattern. After 1 week all genes of interest, except a *Chitin-binding* gene, showed differential expression between control and damaged treatments. After 1 month, six of the genes were differentially expressed and after 2 months only four on the genes were differentially expressed.

3.2. Experiment two: localisation of damage response

The response of twelve candidate genes to shell damage was investigated by comparing control and damaged treatments in experiment two (Table 5). Three genes were unresponsive to damage, three genes were significantly up regulated and the remaining six genes were significantly down regulated.

To test if each candidate gene showed a spatial expression pattern across the four mantle regions in response to damage, data within the control and damaged treatments were compared (Fig. 3). In every instance the control treatment showed no significant difference in expression across the four mantle regions. In contrast, in the damaged treatment, seven genes showed a significant spatial difference in expression across the four mantle regions. Each of the seven differentially expressed genes showed the same spatial pattern; a decrease in expression towards the siphon/posterior mantle edge (tissue location 2, Fig. 1) and an increase in expression away from the drilled hole at the foot/anterior edge of the mantle (tissue location 4, Fig. 1).

4. Discussion

4.1. Experiment one: transcriptional profiling of damage response during a time series

Antarctic marine ectotherms are characterised by slow rates of growth, development and metabolism (Peck et al., 2006), therefore it was unsurprising to discover that the transcriptional response of *L. elliptica* to shell damage was a slow process lasting at least 2 months. In a previous pilot study using reproductively mature clams of approximately 10 years age (60 mm ± 2.85 S.E.) and damage inflicted using the same drilling technique, hole occlusion took 4 months (Clark, pers comm). Animals in the present study were smaller (younger at approximately 4–5 years and immature) with thinner shells, and therefore were expected to repair faster. Qualitative analysis of differentially expressed transcripts over the time course showed the highest number occurred after 1 month, and the lowest after 2 months (Table 2).

Table 2
Overall numbers of differentially expressed transcripts between control and damaged treatments at each time point according to DEXUS analysis of transcriptomic data (experiment one). Numbers in **(bold)** refer to annotated genes.

Time point	Number of contigs differentially expressed	Percentage of contigs differentially expressed
1 week	6,046 **(1,453)**	14.1% **(3.39)**
1 month	7,402 **(1,493)**	17.3% **(3.48)**
2 months	2,998 **(676)**	7% **(1.58)**

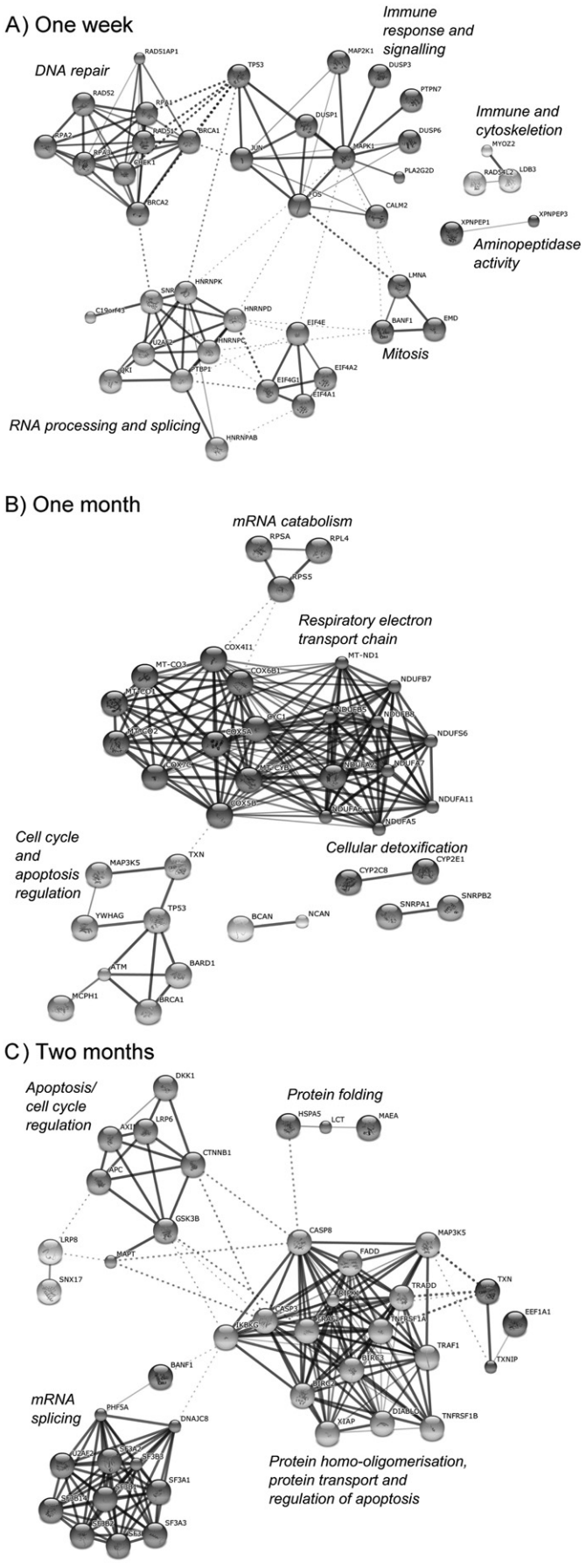

Fig. 2. STRING Database predicted protein-protein interactions for top 50 annotated ($<1e\text{-}^{10}$) differentially expressed contigs between control and damaged treatments in experiment one after A) 1 week B) 1 month and C) 2 months. Clustered using Markov cluster algorithm (MCL), thickness of line indicates strength of interaction, italicized labels indicate most likely biological processes or pathways.

When the twelve candidate transcripts (from experiment two) were highlighted in the DEXUS analysis (Table 4), a decrease in differential expression over time was also observed. The reduction in differential expression over time is coherent with observations of shell occlusion, where the hole had occluded in 2 months in all damaged individuals (Fig. 4). The pattern of differential expression over time was likely due to an initial immune/shock response to the damage, followed by rapid hole-filling, and then a slower response as the shell matrix above the closed hole was filled-in and strengthened. Hence, although there was a qualitative decrease in differential gene expression over time for both the overall differentially expressed transcripts (Table 2) and the twelve transcripts of interest (Table 4), substantial differential expression was still present after 2 months (7% of transcripts were differentially expressed between control and damaged treatments, Table 2), which indicated that shell repair was likely on-going.

Other studies have investigated shell repair in temperate bivalves over various, relatively short, time scales. Clark et al. (2013b) studied *Crassostrea gigas* 1 week after damage, Cho and Jeong (2011) also studied *C. gigas* with three sampling times, 7, 14 and 21 days after injury and, in one of the first documented shell damage-repair experiments, Mount et al. (2004) studied *Crassostrea virginica* only 48 hours after injury. Clark et al. (2013b) observed shell occlusion in all animals after 7 days. Cho and Jeong (2011) also observed occlusion (as a white semi-transparent membrane) which was visible between 24 hours and 4 days after damage. Mount et al. (2004) observed haemocyte mediated hole-filling after 48 hours. The shell repair of other mollusc groups has also been investigated. In a longer-term time scale, Fleury et al. (2008) damaged *Haliotis tuberculata* shells and studied mantle histology 7, 14, 30 and 60 days after injury. Fleury and colleagues conclude the hole was occluded by a brownish organic lamella, which resembled a periostracal layer, after 1 day. In the present study, however, only half the damaged animals showed partial occlusion after 1 week and it took 1 month before all animals sealed the hole (Fig. 4). As the present study used three time points spread over 2 months, data on the exact time and rate of occlusion were unattainable, but the occlusion process took a minimum of twice as long in the Antarctic clam compared to temperate molluscs.

Similar to the present study, Husmann et al. (2014) investigated transcriptional responses to shell damage in *L. elliptica* by collecting siphon and haemocyte samples 2 and 21 days post-injury. Shell damage was inflicted using a wrench and was a blunt, crushing motion. Husmann and colleagues did not report transcriptional differences between control and damaged groups over time, but instead their main findings were regarding effects of age and starvation on the ability for animals to repair. The present study however, demonstrates that 21 days is perhaps an insufficient time period to study Antarctic shell repair. Transcriptional responses to damage have also been studied in non-mollusc species. In a microarray experiment investigating scale regeneration (a type of biomineralisation) in sea bream, Vieira et al. (2011) found 769 differentially expressed genes after 3 days but only 21 differentially expressed after 7 days. Taken together with the results of the present study, damage-repair experiments emphasise the importance of timing in biomineralisation studies.

Qualitative analysis of the differential genes expressed between control and damaged treatments highlights the different biological processes that are likely to be important at different time scales (Fig. 2). The qualitative STRING analysis provides a visual tool to consider processes which are important at different stages of the damage-repair process. It does however, have some limitations. Firstly, the annotations used have to be from the human Uniprot database, therefore mollusc specific

Table 3
The differential expression status between control and damaged treatments of "classic" biomineralisation genes at each time point according to DEXUS analysis of transcriptomic data (experiment one). Contig ID of *Pif* different to Table 4 due to multiple copies of *Pif-like* genes in the *L. elliptica* transcriptome.

	1 week		1 month		2 months	
Contig I.D./description	Comparison	*I/NI* value	Comparison	*I/NI* value	Comparison	*I/NI* value
18958277/Pif	Unchanged	3.18e-14	Unchanged	1.17e-06	**Different**	**1.16**
CL767/Nacrein-like 3	Unchanged	4.83e-08	Unchanged	6.49e-08	Unchanged	1.03e-07
18941698/Perlucin	Unchanged	3.10e-05	Unchanged	7.15e-06	Unchanged	0.001
18977631/PfN44	Unchanged	7.93e-06	**Different**	**0.42**	Unchanged	2.16e-14
18956919/Chitin synthase	Unchanged	1.94e-14	Unchanged	2.23e-07	**Different**	**1.14**
18934508/Dentin matrix protein	Unchanged	0.0003	Unchanged	1.74e-06	Unchanged	0.0014
18972263/Insoluble matrix shell protein	**Different**	**0.74**	Unchanged	8.27e-15	Unchanged	8.88e-05

proteins, such as shell biomineralisation proteins will not be identified. Secondly, only proteins which interact are included in analysis; it is possible that key processes are only represented by a single, non-interacting hit in the top 50 annotated differentially expressed contigs. To supplement the STRING analyses Blastx against the entire NCBI nr database (Supplementary Table 1, 2 and 3) was also carried out. Although many of the annotations were conserved using both methods, some notable differences were identified.

4.1.1. 1 week after damage

In the immediate short-term after damage (1 week) STRING analysis highlighted differences between control and damaged treatments in typical stress responses such as: immune system activation, signalling, cytoskeleton processes and DNA repair (Tomanek, 2011). The immune response was unsurprising as the external barrier of the animals was breached, allowing ingress of pathogens and potential infection. It is likely the primary response was to combat disease and seal the hole. The cytoskeleton has a role not only in morphological restructuring (such as cell proliferation) and intracellular protein transport, but also in the stress response (Wang et al., 2009).

At the 1 week time point, the full NCBI nr annotation of differentially expressed transcripts highlighted additional transcripts of interest which were unresolved in the STRING analysis (Supplementary Table 1). Notably two transcripts that were likely to represent the activation of biomineralisation processes to occlude the hole: *Calmodulin* and *Fibulin-2*. Yan et al., 2007 demonstrated that Calmodulin and Calmodulin-like proteins modify the morphology of calcite and aragonite crystals *in vitro*. Calmodulin proteins have also been localised in the extracellular matrix of both prismatic and nacreous shell layers. Fibulins are a diverse family of extracellular matrix proteins, and Fibulin-2 specifically contributes to elasticity of matrices (Timpl et al., 2003). Fibulins, so far, are uncharacterised in terms of any potential role in mollusc biomineralisation. Arany et al., 2009 however, show that Fibulin is involved in the biomineralisation of mouse odontoblast cells. Only one candidate "classic" biomineralisation gene *(Insoluble shell matix protein*) was differentially expressed after 1 week (Table 3), highlighting that the "classic" genes are not an exclusive set of molecules involved in biomineralisation, but are rather likely to be part of a more complex pathway or network.

4.1.2. 1 month after damage

One month after damage, STRING analysis detected a major difference in respiratory electron transport chain processes between damaged and control treatments (Fig. 2). Biomineralisation, and specifically the production of extracellular matrix proteins, is costly (Day et al., 2000; Palmer, 1983). The difference in respiration between treatments is likely due to the energetic requirements for shell repair (and possible tissue repair). Other differentially expressed processes included: mRNA catabolism, cell cycle/apoptosis regulation and cellular

Table 5
Expression response of twelve candidate genes to damage during spatial localisation experiment (experiment two). Comparison between control and damaged treatments using Kruskal–Wallis one-way analysis of variance by ranks to test for up or down regulation.

Contig I.D.; description	H	*df*	P	Response to damage across whole mantle
Contig 02037; Astacin-like	0.71	1	0.4	No change
Contig 00332; Pif	30.3	1	<0.001	↓ Down regulated
Contig 01359; Tyrosinase B	25.04	1	<0.001	↑ Up regulated
Contig 01311; Shell matrix protein	0.08	1	0.772	No change
Contig 01785; Mytilin	6.39	1	0.011	↑ Up regulated
Contig 00041; Chitin-binding peritrophin	6.35	1	0.012	↓ Down regulated
Contig 01043; Unknown	41.32	1	<0.001	↓ Down regulated
Contig 01663; Tyrosinase A	25.2	1	<0.001	↓ Down regulated
Contig 18937102; Chitinase	NA	NA	NA	No change
Contig 1586; Tyrosine	34.93	1	<0.001	↓ Down regulated
Contig 2930; Unknown	13.82	1	<0.001	↑ Up regulated
Contig 3459; Unknown	52.23	1	<0.001	↓ Down regulated

Table 4
The differential expression status (between control and damaged treatments) of twelve candidate genes of interest, over time, according to DEXUS analysis of transcriptomic data (experiment one). Genes highlighted in **bold** failed to show time-dependant expression patterns.

	1 Week		1 Month		2 Months	
Contig I.D./description	Comparison	*I/NI* value	Comparison	*I/NI* value	Comparison	*I/NI* value
Contig 02037; Astacin-like	Different	0.331415	Different	0.250723	Unchanged	0.059722
Contig 00332; Pif	Different	0.137805	Different	0.252471	Unchanged	0.099168
Contig 01359; Tyrosinase B	Different	0.33538	Different	0.165317	Unchanged	2.50E-13
Contig 01311; Shell matrix protein	Different	0.378735	Unchanged	0.029765	Different	0.115359
Contig 01785; Mytilin	Different	0.132645	Different	0.17044	Unchanged	5.43E-13
Contig 00041; Chitin-binding peritrophin	**Unchanged**	**0.061946**	**Unchanged**	**1.53E-13**	**Unchanged**	**4.61E-13**
Contig 01043; Unknown	Different	0.127414	Different	0.307574	Unchanged	0.08005
Contig 01663; Tyrosinase A	Different	0.251336	Unchanged	0.078672	Unchanged	0.025998
Contig 18937102; Chitinase	Different	0.945757	Unchanged	4.29E-06	Different	0.692891
Contig 1586; Tyrosine	Different	0.865892	Unchanged	1.06E-09	Unchanged	2.86E-05
Contig 2930; Unknown	**Different**	**2.409681**	**Different**	**0.420453**	**Different**	**1.528578**
Contig 3459; Unknown	Different	2.328701	Unchanged	7.92E-08	Different	1.34395
Number of differentially expressed	11		6		4	

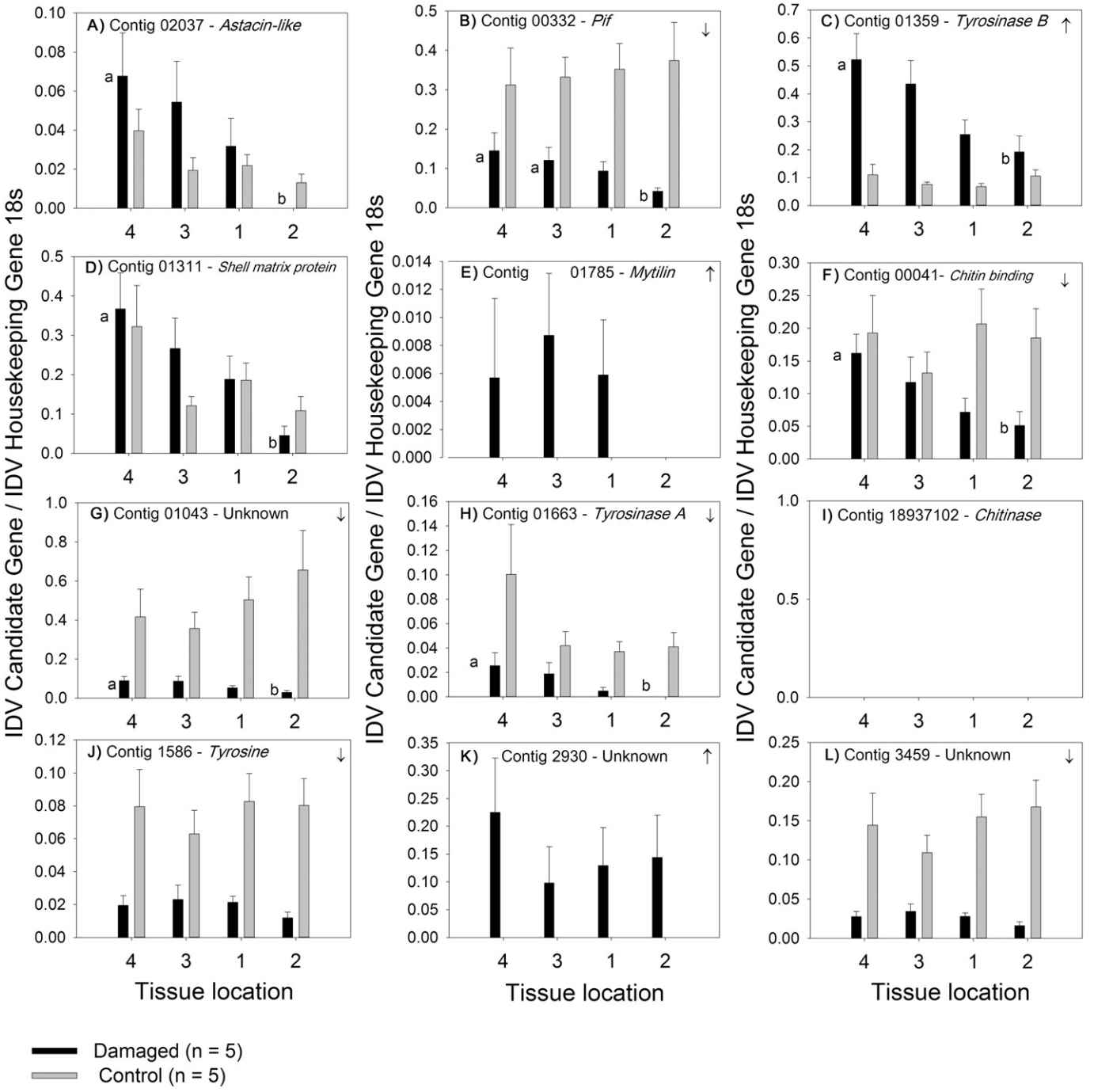

Fig. 3. Expression of twelve candidate genes across four tissue locations in experiment two as determined by semi-quantitative PCR (mean ± S.E. n = 5). Statistically significant differences *within* treatments (across locations) indicated by different letters above bars. Statistically significant differences *between* treatments (up↑ or down↓ regulation between damaged vs control) indicated by arrow in top of plot.

detoxification. The differences observed in mRNA catabolism and cell cycle/apoptosis regulation could represent the re-configuring of cellular processes, from stress response to energy production required for repair. The differences in cellular detoxification between treatments could be linked to oxidative stress. Damaged animals were likely to be experiencing oxidative stress for two reasons: increased aerobic respiration and the macrophages oxidative burst during immune response. STRING identified changes in the cytochrome P450 system, which is known to be involved in mediating oxidative stress (Lingappan et al., 2014). In addition, the full NCBI nr annotation of the differentially expressed transcripts (Supplementary Table 2) included *Thioredoxin,* which is involved in cellular redox homeostasis (Jones and Go, 2010).

At the 1 month time point, STRING analysis and the full NCBI nr annotations failed to highlight a biomineralisation signal (Fig. 2; Table 3; Supplementary Table 2). Only one candidate "classic" biomineralisation gene (*PfN44*) was differentially expressed. At this time point all the damaged shells had occluded and the initial stress of a breach to the external barrier was resolved. It is possible that biomineralisation to fill in the hole (mineralise the occluded layer) had not started, and instead animals were reallocating cellular energy before biomineralisation could commence.

4.1.3. 2 months after damage

After 2 months, the STRING analysis revealed differences in protein transport and turn-over, protein folding, mRNA splicing and

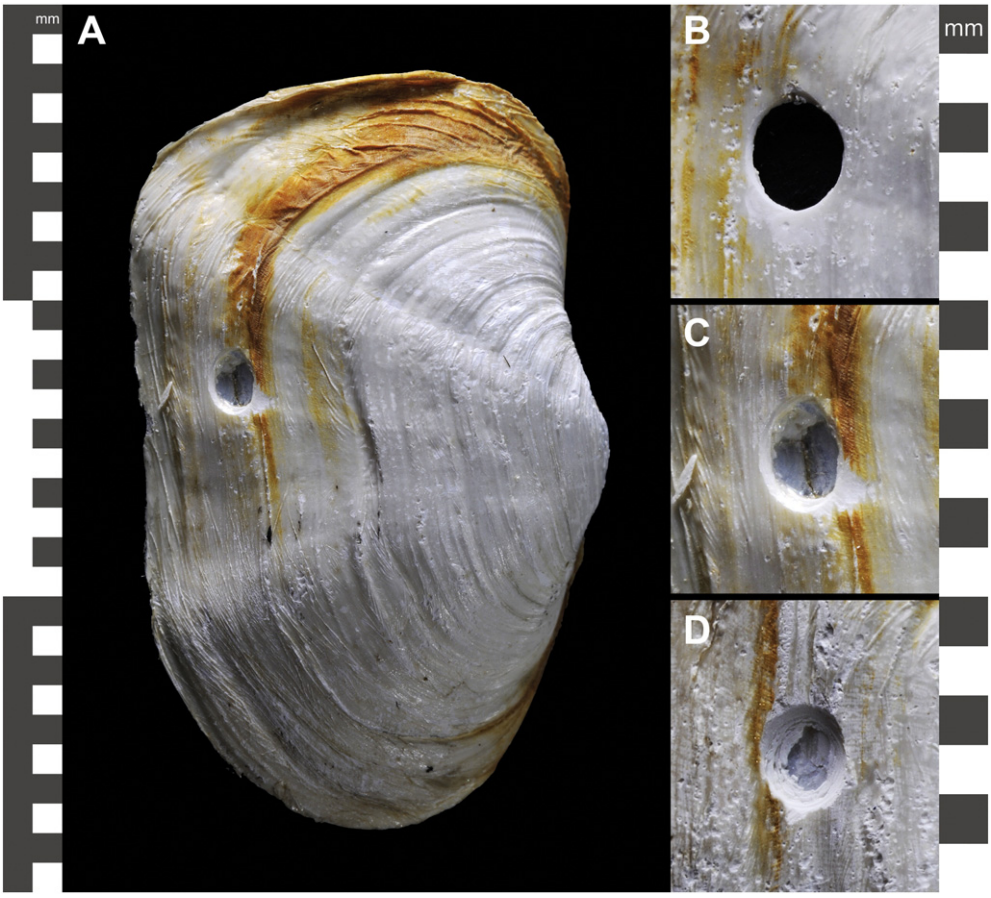

Fig. 4. Photographs of damage-repair in *L. elliptica* at each time point during time series. A) Example of a damaged shell, scale bar to left of image. Zoomed in photos of damage-repair B) 1 week, C) 1 month and D) 2 months after damage, scale bar on the right of images.

cell cycle/apoptosis regulation (Fig. 2). Protein turn-over indicated that the mantle tissue was metabolically active, with increased cell turnover potentially due to tissue remodelling in response to the damage.

Although the STRING analysis was unable to detect a biomineralisation signal at 2 months, the full NCBI nr annotation of the differentially expressed transcripts (Supplementary Table 3) highlighted four genes potentially involved in the production of the proteinaceaous extracellular matrix component of the shell: *Collagen* (Benson et al., 1986), *Calmodulin* (Fang et al., 2008), *Fibrinogen* (Fang et al., 2011) and *Low-density lipoprotein receptor* (Leupin et al., 2011). In addition, two candidate "classic" biomineralisation transcripts (*Pif* and *Chitin synthase*) were differentially expressed (Table 3). The differential expression of biomineralisation transcripts between control and damaged treatments strongly supported the hypothesis that shell repair processes were on-going after 2 months.

4.2. Experiment two: localisation of damage response

Presented here is the first investigation into the spatial molecular response of molluscs to shell damage in mantle tissue. Genes differed in response to shell damage on a spatial scale and surprisingly, there was no peak in expression directly below the drilled hole (Fig. 3). A consistent spatial expression pattern emerged for seven of the twelve genes investigated; a decrease in expression towards the siphon/posterior mantle edge and an increase in expression away from the drilled hole at the foot/anterior edge of the mantle. Currently, the reason for the observed spatial pattern can only be speculated. Mantle tissue can be functionally divided into at least three zones responsible for secreting nacre, prisms or periostracum (Fang et al., 2011; Gardner et al., 2011; Jolly et al., 2004; Sato et al., 2013; Suzuki et al., 2004); the expression of certain genes in each zone may be pre-programmed despite the influence of injury. Or, the expression pattern may be linked to the close proximity of the foot which protrudes outside the mantle when in use. One hypothesis could be that the anterior region of the mantle edge is more sensitive to damage and therefore has a higher induced response than other regions. The anterior region of the shell is the leading edge which buries into sediment and is where the foot protrudes. The movement of the foot in and out of the pallial space, coupled with burying into the sediment, could make anterior region of the shell more susceptible to damage and therefore more sensitive.

Three candidate genes were up regulated in response to shell damage (contig 01359 – *Tyrosinase B*, contig 01785 – *Mytilin* and contig 2930 – unknown; Table 5). Two of the up regulated genes, *Mytilin* and an unknown gene, showed no spatial pattern and were ubiquitously increased across the mantle edge. Mytilin is an anti microbial peptide isolated from a marine mussel which is synthesised in, and transported by, haemocytes (Mitta et al., 2000). Mitta et al., 2000 found no expression of *Mytilin* in the mantle tissue of *Mytilus galloprovincialis*. It is likely the up regulation and ubiquitous expression of *Mytilin* detected in the present study was due to an infiltration of haemocytes into the mantle tissue as part of the immune response to injury. The spatial expression pattern shows that the *Mytilin* immune response is unspecific to the injury site. On the other hand, *Tyrosinase B* - contig 01359, was up regulated with a specific spatial pattern in relation to the injury site. Tyrosinase is involved in cross-linking of the periostracum, forming an insoluble outer layer protecting the shell; it is also involved in the

pigmentation and formation of prismatic shell layers (Waite et al., 1979; Zhang et al., 2006). Tyrosinase is therefore a structural matrix protein which plays a role in both repair and normal shell growth. Several mollusc species have multiple paralogues of the *Tyrosinase* gene and it is thought different copies have evolved different functional roles due to sub-functionalisation of the duplicated genes, allowing persistence of both copies (Force et al., 1999). *L. elliptica* have two copies of *Tyrosinase* (*A & B*) with only one of these expressed in response to shell damage (Aguilera et al., 2014; Clark et al., 2010; Huning et al., 2013; Luna-Acosta et al., 2011). Similar to the present study, Huning et al. (2013) found only one of the two *Mytilus edulis Tyrosinase* paralogues was responsive to shell damage.

Three candidate genes were unresponsive to damage (contig 02037 – *Astacin-like*, contig 01331 – *Shell matrix protein* and contig 183937 – *Chitinase*; Table 5). *Chitinase* expression was not detected in the control or damaged treatment at any mantle region (Fig. 3I). The negative *Chitinase* result could infer that *Chitinase* is uninvolved in shell repair after 1 week; however, in experiment one, at 1 week in the time-series, *Chitinase* showed significant up regulation and hence was selected for further localisation in experiment two (Table 4). The function of Chitinase and Chitinase-like proteins have been investigated in arthropods with chitinous exoskeletons; they are typically involved in moult-cycles, wound healing and tissue repair (Bonneh-Barkay et al., 2010; Chen et al., 2004). Previous work showed *Chitinase* expression is up regulated in response to injury after 21 days in young, but not old, *L. elliptica* (Husmann et al., 2014), as well as in the oyster *Crassostrea gigas* (Badariotti et al., 2007). Clark et al., 2013a also found age to be a significant factor when investigating responses to hypoxia in *L. elliptica*. It is possible the present study found differential expression of certain genes, such as *Chitinase*, in experiment one, but not two, because the size and age of the animals were different in the two experiments. The genes coding for an Astacin-like and Shell matrix protein were neither up nor down regulated in response to damage, however both showed a significant spatial expression pattern in the damaged treatment, which was absent in the controls (Fig. 3A & D). Despite the lack of up or down regulation, the presence of a spatial pattern in the damaged but not control treatment represents the likely reconfiguration of molecular events across the mantle.

Six candidate genes were down regulated in response to damage (contig 1586 – *Tyrosine*, contig 3459 – unknown, contig 00332 – *Pif*, contig 01043 – unknown, contig 00041 – *Chitin-binding peritrophin* and contig 01663 – *Tyrosinase A*; Table 5). Two of the down regulated genes, *Tyrosine* and an unknown gene, showed no spatial pattern and were ubiquitously decreased across the mantle edge. The remaining four genes – *Pif*, *Chitin-binding peritrophin*, an unknown gene and *Tyrosinase A* – were down regulated with a specific spatial pattern in relation to the damage site. Similar to the results discussed above, the spatial patterns observed are likely to represent the movement of cellular processes and functional zonation in the mantle.

4.3. Conclusions and recommendations

In experiment one, the transcriptional profiling of damage response over time in the Antarctic clam *Laternula elliptica,* shell repair was revealed to be a slow process lasting at least 2 months. Results highlighted different biological processes were important at different time scales during repair, thus enabling more targeted analyses in the future. For example, more sampling time points around the immediate short-term (e.g. 1–7 days) would provide a better understanding of the interaction between the immune, stress and biomineralisation response. In addition, around 1 month after damage there appears to be a switch from energy production to biomineralisation, which is a critical step. Longer experiments are also needed to fully characterise the biomineralisation component of the shell repair. As the time-scale of shell repair is unknown for most species, preliminary studies such as the one detailed here, provide a cost-effective approach to discover the most important molecular time-scales for the species being investigated. Knowledge on time-scales maximises sampling efficiency, as well as minimising sequencing costs; a particularly important factor for slow growing animals with enhanced longevity, such as those inhabiting the Southern Ocean, where biological processes are slow and age is a significant factor in response timings.

Although some biomineralisation signal was detected in the transcriptional profiling experiment, the signal was not dominant over other biological processes and the "classical" biomineralisation candidate genes were largely unchanged overtime. In order to better characterise and understand the molluscan biomineralisation pathway, the regulation of genes with the same expression pattern as "classic" biomineralisation genes should be investigated. Methods such as gene-network and co-regulation analysis could lead to the identification of novel genes and a better understanding on how biomineralisation genes interact forming a coherent pathway.

Experiment two highlighted the spatial localisation of repair mechanisms, different genes showed different spatial patterns in relation to a single drilled hole. The spatial pattern revealed is important for all future damage-repair experiments as the location and number of holes, in relation to where the underlying tissue is sampled from, could bias transcriptomic results. Future work investigating damage-repair mechanisms should drill several holes around the edge of the shell in order to stimulate expression across the entire mantle edge and maximise the tissue samples that can be taken for analysis, knowing that expression is homogeneous across all samples.

The present pilot experiment generated valuable data on the temporal and spatial response of shell damage-repair and therefore provides a baseline not only for future studies in *L. elliptica,* but also other molluscs.

Supplementary data to this article can be found online at http://dx.doi.org/10.1016/j.margen.2015.01.009.

Acknowledgements

VAS was funded by a NERC DTG studentship (Project Reference: NE/J500173/1) to the British Antarctic Survey. MSC, MAST and LSP were financed by NERC core funding to the British Antarctic Survey, Polar Sciences for Planet Earth Programme. We would like to thank Laura J. Weir for technical assistance and Elizabeth M. Harper for advice on shell structure and repair processes. We thank the dive team at Rothera research station, Antarctica for support in animal collection. Diving oversight was provided by the NERC National Centre for Scientific Diving, Oban.

References

Aguilera, F., McDougall, C., Degnan, B.M., 2014. Evolution of the tyrosinase gene family in bivalve molluscs: Independent expansion of the mantle gene repertoire. Acta Biomater. 10, 3855–3865.

Altschul, S.F., Gish, W., Miller, W., Myers, E.W., Lipman, D.J., 1990. Basic local alignment search tool. J. Mol. Biol. 215, 403–410.

Appeltans, W., Ahyong, S.T., Anderson, G., Angel, M.V., Artois, T., Bailly, N., Bamber, R., Barber, A., Bartsch, I., Berta, A., Blazewicz-Paszkowycz, M., Bock, P., Boxshall, G., Boyko, C.B., Brandao, S.N., Bray, R.A., Bruce, N.L., Cairns, S.D., Chan, T.Y., Cheng, L.N., Collins, A.G., Cribb, T., Curini-Galletti, M., Dahdouh-Guebas, F., Davie, P.J.F., Dawson, M.N., De Clerck, O., Decock, W., De Grave, S., de Voogd, N.J., Domning, D.P., Emig, C.C., Erseus, C., Eschmeyer, W., Fauchald, K., Fautin, D.G., Feist, S.W., Fransen, C., Furuya, H., Garcia-Alvarez, O., Gerken, S., Gibson, D., Gittenberger, A., Gofas, S., Gomez-Daglio, L., Gordon, D.P., Guiry, M.D., Hernandez, F., Hoeksema, B.W., Hopcroft, R.R., Jaume, D., Kirk, P., Koedam, N., Koenemann, S., Kolb, J.B., Kristensen, R.M., Kroh, A., Lambert, G., Lazarus, D.B., Lemaitre, R., Longshaw, M., Lowry, J., Macpherson, E., Madin, L.P., Mah, C., Mapstone, G., McLaughlin, P.A., Mees, J., Meland, K., Messing, C.G., Mills, C.E., Molodtsova, T.N., Mooi, R., Neuhaus, B., Ng, P.K.L., Nielsen, C., Norenburg, J., Opresko, D.M., Osawa, M., Paulay, G., Perrin, W., Pilger, J.F., Poore, G.C.B., Pugh, P., Read, G.B., Reimer, J.D., Rius, M., Rocha, R.M., Saiz-Salinas, J.I., Scarabino, V., Schierwater, B., Schmidt-Rhaesa, A., Schnabel, K.E., Schotte, M., Schuchert, P., Schwabe, E., Segers, H., Self-Sullivan, C., Shenkar, N., Siegel, V., et al., 2012. The magnitude of global marine species diversity. Curr. Biol. 22, 2189–2202.

Arany, S., Koyota, S., Sugiyama, T., 2009. Nerve growth factor promotes differentiation of odontoblast-like cells. J. Cell. Biochem. 106, 539–545.

Arnaud-Haond, S., Goyard, E., Vonau, V., Herbaut, C., Prou, J., Saulnier, D., 2007. Pearl formation: Persistence of the graft during the entire process of biomineralization. Mar. Biotechnol. 9, 113–116.

Arntz, W.E., Brey, T., Gallardo, V.A., 1994. Antarctic Zoobenthos: Oceanography and Marine Biology, Vol 32: an Annual Review. 32, 241–304.

Badariotti, F., Thuau, R., Lelong, C., Dubos, M.P., Favrel, P., 2007. Characterization of an atypical family 18 chitinase from the oyster *Crassostrea gigas*: Evidence for a role in early development and immunity. Dev. Comp. Immunol. 31, 559–570.

Benson, S.C., Benson, N.C., Wilt, F., 1986. The organic matrix of the skeletal spicule of sea-urchin embryos. J. Cell Biol. 102, 1878–1886.

Bonneh-Barkay, D., Zagadailov, P., Zou, H.C., Niyonkuru, C., Figley, M., Starkey, A., Wang, G.J., Bissel, S.J., Wiley, C.A., Wagner, A.K., 2010. YKL-40 expression in traumatic brain injury: An initial analysis. J. Neurotrauma 27, 1215–1223.

Chen, L., Wu, W., Dentchev, T., Zeng, Y., Wang, J.H., Tsui, I., Tobias, J.W., Bennett, J., Baldwin, D., Dunaief, J.L., 2004. Light damage induced changes in mouse retinal gene expression. Exp. Eye Res. 79, 239–247.

Cho, S.-M., Jeong, W.-G., 2011. Prismatic shell repairs by hemoctyes in the extrapallial fluid of the Pacific Oyster, *Crassostrea gigas*. Korean J. Malacology 27, 223–228.

Clark, M.S., Thorne, M.A.S., Vieira, F.A., Cardoso, J.C.R., Power, D.M., Peck, L.S., 2010. Insights into shell deposition in the Antarctic bivalve *Laternula elliptica*: gene discovery in the mantle transcriptome using 454 pyrosequencing. BMC Genomics 11.

Clark, M.S., Thorne, M.A.S., Amaral, A., Vieira, F., Batista, F.M., Reis, J., Power, D.M., 2013a. Identification of molecular and physiological responses to chronic environmental challenge in an invasive species: the Pacific oyster, *Crassostrea gigas*. Ecol. Evol. 3, 3283–3297.

Clark, M.S., Husmann, G., Thorne, M.A.S., Burns, G., Truebano, M., Peck, L.S., Abele, D., Philipp, E.E.R., 2013b. Hypoxia impacts large adults first: consequences in a warming world. Glob. Chang. Biol. 19, 2251–2263.

Cook, A.J., Fox, A.J., Vaughan, D.G., Ferrigno, J.G., 2005. Retreating glacier fronts on the Antarctic Peninsula over the past half-century. Science 308, 541–544.

Day, E.G., Branch, G.M., Viljoen, C., 2000. How costly is molluscan shell erosion? A comparison of two patellid limpets with contrasting shell structures. J. Exp. Mar. Biol. Ecol. 243, 185–208.

de Paula, S.M., Silveira, M., 2009. Studies on molluscan shells: Contributions from microscopic and analytical methods. Micron 40, 669–690.

Fang, Z., Yan, Z., Li, S., Wang, Q., Cao, W., Xu, G., Xiong, X., Xie, L., Zhang, R., 2008. Localization of calmodulin and calmodulin-like protein and their functions in biomineralization in *P. fucata*. Prog. Nat. Sci.: Mater. Int. 18, 405–412.

Fang, D., Xu, G., Hu, Y., Pan, C., Xie, L., Zhang, R., 2011. Identification of genes directly involved in shell formation and their functions in pearl oyster, *Pinctada fucata*. Plos ONE 6.

Fleury, C., Marin, F., Marie, B., Luquet, G., Thomas, J., Josse, C., Serpentini, A., Lebel, J.M., 2008. Shell repair process in the green ormer *Haliotis tuberculata*: A histological and microstructural study. Tissue Cell 40, 207–218.

Force, A., Lynch, M., Pickett, F.B., Amores, A., Yan, Y.L., Postlethwait, J., 1999. Preservation of duplicate genes by complementary, degenerative mutations. Genetics 151, 1531–1545.

Franceschini, A., Szklarczyk, D., Frankild, S., Kuhn, M., Simonovic, M., Roth, A., Lin, J.Y., Minguez, P., Bork, P., von Mering, C., Jensen, L.J., 2013. STRING v9.1: protein-protein interaction networks, with increased coverage and integration. Nucleic Acids Res. 41, D808–D815.

Freer, A., Bridgett, S., Jiang, J.H., Cusack, M., 2014. Biomineral proteins from *Mytilus edulis* mantle tissue transcriptome. Mar. Biotechnol. 16, 34–45.

Gardner, L.D., Mills, D., Wiegand, A., Leavesley, D., Elizur, A., 2011. Spatial analysis of biomineralization associated gene expression from the mantle organ of the pearl oyster *Pinctada maxima*. BMC Genomics 12.

Gazeau, F., Parker, L.M., Comeau, S., Gattuso, J.-P., O'Connor, W.A., Martin, S., Poertner, H.-O., Ross, P.M., 2013. Impacts of ocean acidification on marine shelled molluscs. Mar. Biol. 160, 2207–2245.

Harper, E.M., Clark, M.S., Hoffman, J.I., Philipp, E.E.R., Peck, L.S., Morley, S.A., 2012. Iceberg scour and shell damage in the Antarctic bivalve *Laternula elliptica*. Plos ONE 7.

Huning, A., Melzner, F., Thomsen, J., Gutowska, M.A., Kramer, L., Frickenhaus, S., Rosenstiel, P., Portner, H.O., Philipp, E.E.R., Lucassen, M., 2013. Impacts of seawater acidification on mantle gene expression patterns of the Baltic Sea blue mussel: implications for shell formation and energy metabolism. Mar. Biol. 160, 1845–1861.

Husmann, G., Abele, D., Rosenstiel, P., Clark, M.S., Kraemer, L., Philipp, E.E.R., 2014. Age-dependent expression of stress and antimicrobial genes in the hemocytes and siphon tissue of the Antarctic bivalve, *Laternula elliptica*, exposed to injury and starvation. Cell Stress Chaperones 19, 15–32.

Jolly, C., Berland, S., Milet, C., Borzeix, S., Lopez, E., Doumenc, D., 2004. Zonal localization of shell matrix proteins in mantle of *Haliotis tuberculata* (Mollusca, Gastropoda). Mar. Biotechnol. 6, 541–551.

Jones, D.P., Go, Y.M., 2010. Redox compartmentalization and cellular stress. Diabetes Obes. Metab. 12, 116–125.

Joubert, C., Piquemal, D., Marie, B., Manchon, L., Pierrat, F., Zanella-Cleon, I., Cochennec-Laureau, N., Gueguen, Y., Montagnani, C., 2010. Transcriptome and proteome analysis of *Pinctada margaritifera* calcifying mantle and shell: Focus on biomineralization. BMC Genomics 11.

Klambauer, G., Unterthiner, T., Hochreiter, S., 2013. DEXUS: identifying differential expression in RNA-Seq studies with unknown conditions. Nucleic Acids Res. 41.

Leupin, O., Piters, E., Halleux, C., Hu, S., Kramer, I., Morvan, F., Bouwmeester, T., Schirle, M., Bueno-Lozano, M., Fuentes, F.J.R., Itin, P.H., Boudin, E., de Freitas, F., Jennes, K., Brannetti, B., Charara, N., Ebersbach, H., Geisse, S., Lu, C.X., Bauer, A., Van Hul, W., Kneissel, M., 2011. Bone overgrowth-associated mutations in the LRP4 gene impair sclerostin facilitator function. J. Biol. Chem. 286, 19489–19500.

Li, H., Ruan, J., Durbin, R., 2008. Mapping short DNA sequencing reads and calling variants using mapping quality scores. Genome Res. 18, 1851–1858.

Lingappan, K., Jiang, W.W., Wang, L.H., Wang, G.D., Couroucli, X.I., Shivanna, B., Welty, S.E., Barrios, R., Khan, M.F., Nebert, D.W., Roberts, L.J., Moorthy, B., 2014. Mice deficient in the gene for cytochrome P450 (CYP)1A1 Are more susceptible than wild-type to hyperoxic lung injury: Evidence for protective role of CYP1A1 against oxidative stress. Toxicol. Sci. 141.

Luna-Acosta, A., Thomas-Guyon, H., Amari, M., Rosenfeld, E., Bustamante, P., Fruitier-Arnaudin, I., 2011. Differential tissue distribution and specificity of phenoloxidases from the Pacific oyster *Crassostrea gigas*. Comp. Biochem. Physiol. B Biochem. Mol. Biol. 159, 220–226.

Luo, R., Liu, B., Xie, Y., Li, Z., Huang, W., Yuan, J., He, G., Chen, Y., Pan, Q., Liu, Y., Tang, J., Wu, G., Zhang, H., Shi, Y., Liu, Y., Yu, C., Wang, B., Lu, Y., Han, C., Cheung, D.W., Yiu, S.M., Peng, S., Xiaoqian, Z., Liu, G., Liao, X., Li, Y., Yang, H., Wang, J., Lam, T.W., Wang, J., 2012. SOAPdenovo2: an empirically improved memory-efficient short-read de novo assembler. Gigascience 1, 18.

Lydeard, C., Cowie, R.H., Ponder, W.F., Bogan, A.E., Bouchet, P., Clark, S.A., Cummings, K.S., Frest, T.J., Gargominy, O., Herbert, D.G., Hershler, R., Perez, K.E., Roth, B., Seddon, M., Strong, E.E., Thompson, F.G., 2004. The global decline of nonmarine mollusks. Bioscience 54, 321–330.

Marie, B., Joubert, C., Tayale, A., Zanella-Cleon, I., Belliard, C., Piquemal, D., Cochennec-Laureau, N., Marin, F., Gueguen, Y., Montagnani, C., 2012. Different secretory repertoires control the biomineralization processes of prism and nacre deposition of the pearl oyster shell. Proceedings of the National Academy of Sciences of the United States of America. vol. 109, pp. 20986–20991.

Marie, B., Jackson, D.J., Ramos-Silva, P., Zanella-Cleon, I., Guichard, N., Marin, F., 2013. The shell-forming proteome of *Lottia gigantea* reveals both deep conservations and lineage-specific novelties. FEBS J. 280, 214–232.

McNeil, B.I., Matear, R.J., 2008. Southern Ocean acidification: A tipping point at 450-ppm atmospheric CO(2). Proceedings of the National Academy of Sciences of the United States of America. vol. 105.

Meenakshi, V.R., Hare, P.E., Wilbur, K.M., 1971. Amino acids of the organic matrix of neogastropod shells. Comp. Biochem. Physiol. B Comp. Biochem. 40, 1037–1043.

Meldrum, F.C., 2003. Calcium carbonate in biomineralisation and biomimetic chemistry. Int. Mater. Rev. 48, 187–224.

Mitta, G., Vandenbulcke, F., Hubert, F., Salzet, M., Roch, P., 2000. Involvement of mytilins in mussel antimicrobial defense. J. Biol. Chem. 275, 12954–12962.

Miyamoto, H., Miyoshi, F., Kohno, J., 2005. The carbonic anhydrase domain protein nacrein is expressed in the epithelial cells of the mantle and acts as a negative regulator in calcification in the mollusc *Pinctada fucata*. Zool. Sci. 22, 311–315.

Mount, A.S., Wheeler, A.P., Paradkar, R.P., Snider, D., 2004. Hemocyte-mediated shell mineralization in the eastern oyster. Science 304, 297–300.

Niu, D.H., Wang, L., Sun, F.Y., Liu, Z.J., Li, J.L., 2013. Development of molecular resources for an intertidal clam, *Sinonovacula constricta*, using 454 transcriptome sequencing. Plos ONE 8.

Palmer, A.R., 1983. Relative cost of producing skeletal organic matrix versus calcification: Evidence from marine gastropods. Mar. Biol. 75, 287–292.

Palmer, A.R., 1992. Calcification in marine mollusks – how costly is it. Proceedings of the National Academy of Sciences of the United States of America. vol. 89, pp. 1379–1382.

Peck, L.S., Convey, P., Barnes, D.K.A., 2006. Environmental constraints on life histories in Antarctic ecosystems: tempos, timings and predictability. Biol. Rev. 81, 75–109.

Sato, Y., Inoue, N., Ishikawa, T., Ishibashi, R., Obata, M., Aoki, H., Atsumi, T., Komaru, A., 2013. Pearl microstructure and expression of shell matrix protein genes MSI31 and MSI60 in the pearl sac epithelium of *Pinctada fucata* by in situ hybridization. Plos ONE 8.

Shi, Y., Yu, C., Gu, Z., Zhan, X., Wang, Y., Wang, A., 2013. Characterization of the pearl oyster (*Pinctada martensii*) mantle transcriptome unravels biomineralization genes. Mar. Biotechnol. 15, 175–187.

Suzuki, M., Murayama, E., Inoue, H., Ozaki, N., Tohse, H., Kogure, T., Nagasawa, H., 2004. Characterization of Prismalin-14, a novel matrix protein from the prismatic layer of the Japanese pearl oyster (*Pinctada fucata*). Biochem. J. 382, 205–213.

Timpl, R., Sasaki, T., Kostka, G., Chu, M.L., 2003. Fibulins: A versatile family of extracellular matrix proteins. Nat. Rev. Mol. Cell Biol. 4, 479–489.

Tomanek, L., 2011. Environmental proteomics: Changes in the proteome of marine organisms in response to environmental stress, pollutants, infection, symbiosis, and development. Annu. Rev. Mar. Sci. 3, 373–399.

Turner, J., Barrand, N.E., Bracegirdle, T.J., Convey, P., Hodgson, D.A., Jarvis, M., Jenkins, A., Marshall, G., Meredith, M.P., Roscoe, H., Shanklin, J., French, J., Goosse, H., Guglielmin, M., Gutt, J., Jacobs, S., Kennicutt, M.C., Masson-Delmotte, V., Mayewski, P., Navarro, F., Robinson, S., Scambos, T., Sparrow, M., Summerhayes, C., Speer, K., Klepikov, A., 2014. Antarctic climate change and the environment: an update. Polar Rec. 50, 237–259.

Vermeij, G.J., 2005. Shells inside out: The architecture, evolution and function of shell envelopment in molluscs: Evolving Form and Function. Fossils Dev. 197–221.

Vieira, F.A., Gregorio, S.F., Ferraresso, S., Thorne, M.A.S., Costa, R., Milan, M., Bargelloni, L., Clark, M.S., Canario, A.V.M., Power, D.M., 2011. Skin healing and scale regeneration in fed and unfed sea bream, *Sparus auratus*. BMC Genomics 12.

Waite, J.H., Saleuddin, A.S.M., Andersen, S.O., 1979. Periostracin – soluble precursor of sclerotized periostracum in *Mytilus edulis*-L. J. Comp. Physiol. 130, 301–307.

Wang, P., Bouwman, F.G., Mariman, E.C.M., 2009. Generally detected proteins in comparative proteomics – A matter of cellular stress response? Proteomics 9, 2955–2966.

Weiner, S., Addadi, L., 2011. Crystallization pathways in biomineralization. In: Clarke, D.R., Fratzl, P. (Eds.), Palo Alto, Annual Reviews. Annual Review of Materials Research vol. 41, pp. 21–40.

Weiner, S., Hood, L., 1975. Soluble protein of the organic matrix of mollusk shells: a potential template for shell formation. Science 190, 987–989.

Wilbur, K.M., Saleuddin, A.S.M., 1983. The mollusca: Physiology, part 2. In: Saleuddin, A.S.M., Wilbur, Karl M. (Eds.), Academic Press.

Yan, Z.G., Fang, Z., Ma, Z.J., Deng, J.Y., Shuo, L.A., Xie, L., Zhang, R.Q., 2007. Biomineralization: Functions of calmodulin-like protein in the shell formation of pearl oyster. Biochim. Biophys. Acta Gen. Subj. 1770, 1338–1344.

Zhang, C., Xie, L.P., Huang, J., Chen, L., Zhang, R.Q., 2006. A novel putative tyrosinase involved in periostracum formation from the pearl oyster (*Pinctada fucata*). Biochem. Biophys. Res. Commun. 342, 632–639.

Zhou, Y.J., He, Z.X., Huang, J., Gong, N.P., Yan, Z.G., Liu, X.J., Sun, J.A., Wang, H.Z., Zhang, G.Y., Xie, L.P., Zhang, R.Q., 2010. Cloning and characterization of the activin like receptor 1 homolog (Pf-ALR1) in the pearl oyster, *Pinctada fucata*. Comp. Biochem. Physiol. B Biochem. Mol. Biol. 156, 158–167.